Rev. Roum. Sci. Techn.– Électrotechn. et Énerg.
Vol. **68**, *4*, pp. 394–399, Bucarest, 2023

RED FOX-BASED FRACTIONAL ORDER FUZZY PID CONTROLLER FOR SMART LED DRIVER CIRCUIT

GANGA MURUGAIYAN[1], JASMINE GNANAMALAR[2], MUTHUKUMARAN NARAYANAPERUMAL[3], VELUCHAMY MUTHUVEL[4]

Keywords: High-power light emitting diodes; Transformerless boost converter; Fractional order PID controller; Fuzzy controller; Red fox optimization algorithm.

Recently, traditional lighting has been replaced by high-power LED (HPLED) due to its significant developments, prolonged lifetime, high brightness, high reliability, and high energy efficiency. Even though conventional converters can precisely match each LED's current, they have some limitations when driving a long string of LEDs. To solve this issue, this paper presents a novel red fox optimized fractional order fuzzy PID Controller (RF-FOFPID) based high gain improved transformerless dc-dc (ITDC) boost converter for a smart LED driver circuit with optimal voltage regulation capability. The error bias is increased to zero by applying FOPID to the fuzzy logic-based compensation steps. The Red Fox optimization algorithm is used to adjust the control parameters of the fractional-level fuzzy PID controller with higher precision to solve limited problems with diverse search spaces. The Simulink model of the proposed converter was created using the MATLAB software tool Simulink and compared with controllers using fractional order PID, fuzzy PID, and conventional proportional integral derivative (PID). The results demonstrated that in terms of minimum overshoot, settling time, rise time, and steady-state error, the proposed converter based on RF-FOFPID outperforms current converters in voltage regulation.

1. **INTRODUCTION**

Nowadays, most of the research is focused on energy consumption, and one of the effective ways is by replacing the conventional light source with energy-efficient LED lamps. Since the LED is an efficient luminescent device with suitable bandwidth and high thermal and chemical stability [1]. Hence, LED has ubiquitous applications, such as televisions, smartphones, digital cameras, digital watches, automotive headlamps, luminescent-controlled smart lamps, and so on [2]. In this research work, one of the smart LED control approaches for controlling the driver circuit using an intelligent algorithm is introduced in this article.

The dc-dc buck converter is commonly preferred in LED driver circuits due to its high efficiency and simple circuit topology. However, the buck converter exhibits a discontinuous performance while subjected to exogenous disturbances and unprecedented nonlinearities. These issues are overcome by a closed-loop control scheme with a conventional PID controller [3]. However, tuning the PID controller gain parameters under dynamic situations is challenging, and many metaheuristic methodologies are being proposed in many research articles to achieve this task. To enhance performance further, in recent years, the PID controllers have been replaced with fractional order PID controllers (FOPID), which consist of two additional parameters, such as integrator and derivative orders. The dominance of FOPID over PID controllers in various engineering fields has been successfully proved [4–6]. The FOPID controller is preferred in this research article, and its gain parameters are tuned with a proposed novel RFA-based fuzzy controller. Some research work related to the proposed research problem is presented below.

Most of the earlier research articles reported so far aimed to enhance the performance of buck converters employed in LED driver circuits using pulse width modulation (PWM) approaches [7,8]. Using various techniques based on LED, OLED, and laser light sources, lighting systems must become smarter and actively participate in ADAS systems to ensure safety and visibility. Matrix beams, made up of complex optoelectronics, are an example [9]. The FOPID controller is analyzed with a boost dc–dc converter [10]. The fractional order PID controller has been modified using fuzzy logic. A fuzzy fractional-order PID controller was investigated in this study to reduce idle time and improve closed-loop performance for power control of the induction heating system [11].

An artificial bee colony algorithm (ABC) was introduced to minimize voltage fluctuations [12]. The chaotic-based flower pollination algorithm [13] and an antlion (ALO) [14] based FOPID controller on buck converter results were obtained with minimum error values. In the same way, the Cohort Intelligent Algorithm (CI) was proposed to minimize the voltage error presented in the buck converter [15]. Meanwhile, the superiority of ITSE has been proved with the PSO and ABC approaches [16]. Most of the articles in the literature focus only on reducing voltage errors in static environments. Very few research articles take dynamic conditions into account. While several optimization algorithms have been developed to optimize the power conversion control in LED driver circuits to ensure efficient voltage regulation, new algorithms are constantly being developed to improve performance further. Very little effort has been expended on the stability analysis of the system under consideration.

In this proposed approach, the following research contributions are presented:

- An Improved transformerless dc-dc converter is designed by adding the L2C2D2 network to improve the voltage of the power switch by reducing the voltage gain.
- The Red Fox optimized Fractional Order Fuzzy PID Controller (RF-FOFPID) is fed into the converter to regulate the output voltage.
- The performance of the proposed RF-FOFPID controller-based boost converter is tested under fixed loading conditions and various input voltage conditions in voltage regulation and compared with existing controllers.

[1]Hindusthan College of Engineering and Technology, Coimbatore, India, Email: ganga.bme@hicet.ac.in
[2]PSN College of Engineering and Technology, Tirunelveli, India, Email: jasmine@psncet.ac.in
[3]Sri Eshwar College of Engineering, Coimbatore, India, Email: muthukumaran.n@sece.ac.in
[4] Sethu Institute of Technology, Kariapatti, India. Correspondence address, E-mail: muthuvel@sethu.ac.in

DOI: 10.59277/RRST-EE.2023.68.4.12

The remainder of the article is organized as follows: Section 2 describes the modelling of a transformerless dc-dc boost converter and its operation. The proposed RF-FOFPID-based control strategy and controller designs are advertised in section 3. Section 4 presents results and discussions, followed by a closure summary of the proposed work and the future scope.

2. MODELING OF A TRANSFORMERLESS DC-DC BOOST CONVERTER

This section provides the framework of the expected high voltage boost ITDC converter model. The study proposes a new improved transformerless dc-dc step-up converter (ITDC). This proposed converter is designed by adding the $D_1C_1C_2D_2$ network to a conventional transformerless dc-dc converter circuit [17]. The proposed ITDC converter circuit diagram. Thus, this converter also uses two inductors with the same inductance level (L_1 and L_2), three diodes (D_0, D_1, and D_2), and three capacitors (C_0, C_1, and C_2). Analog control signals are used to operate switches S_1 and S_2 simultaneously. Figure 1 illustrates modes 1 and 2, which are two modes in which the operating modes can be separated.

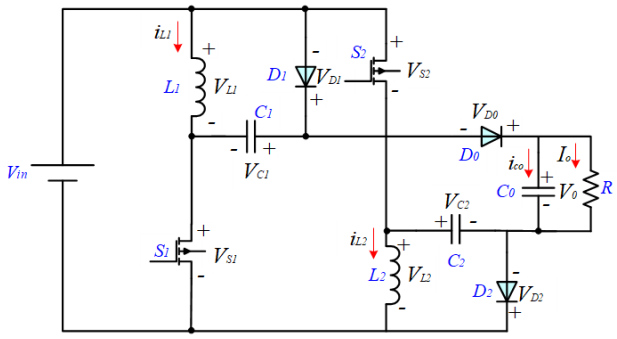

Fig. 1 – Proposed high gain improved transformerless dc-dc converter.

During mode 1 operation, switches S_1 and S_2 are in the ON position. The dc power source charges L_1 and L_2 in parallel, and the load receives the release of the energy contained in the Co. Additionally, there is voltage in L_1, L_2, C_1, and C_2.

$$V_{L1} = V_{L2} = V_{C1} = V_{C2} = V_{in}\,. \quad (1)$$

When operating in mode 2, switches S_1 and S_2 are not used. A series connection is made between source C_C, L_1, C_1, C_2 and L_2 to move current to Co and the load. As a result, the following voltages appear on L1 and L2:

$$V_{L1} = V_{L2} = \frac{V_{in} + V_{c1} + V_{c2} - V_0}{2} = \frac{3V_{in} - V_o}{2}\,. \quad (2)$$

The voltage gain can be calculated from (3) by simplifying it,

$$M_{CCM} = \frac{V_0}{V_{in}} = \frac{3-D}{1-D}\,, \quad (3)$$

where D is the duty cycle.

Generally, the DC input voltage of the converter varies; therefore, to obtain the desired voltage, the average output voltage must be controlled. A desired voltage can be achieved by selecting capacitor C_2,

$$C_2 = \frac{I_{l2} - I_{out}}{V_{C2}}(1-D)T_s\,, \quad (4)$$

where T_s is the time travel.

3. PROPOSED RF-FOFPID-BASED CONTROL STRATEGY

The design problem is as follows: optimize gain values of the FOFPID controller in a closed-loop ITDC converter circuit. The schematic representation of the ITDC converter optimized with the proposed RF-FOFPID controller is depicted in Fig. 2. Initially, the control signals are generated from the fuzzy controller according to the rule-based table corresponding to the input and desired output parameters. Meanwhile, the control signal generated from the FOPID controller while optimizing with the Red Fox algorithm concerning the objective function developed. The consolidated control signals from fuzzy and RF-tuned FOFPID controllers are fed to the converter to regulate the output voltage for High Power LED (HPLED) application.

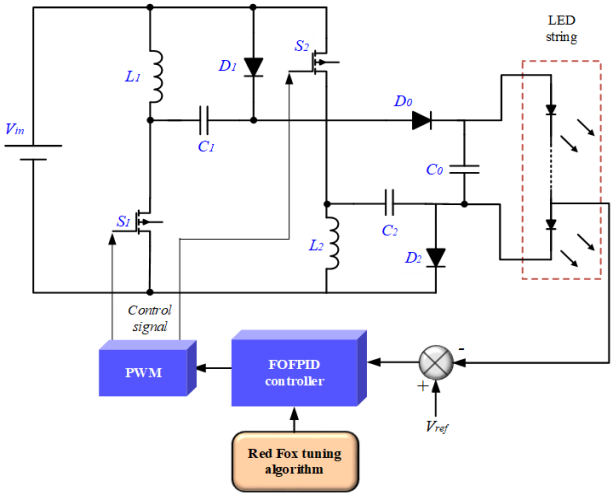

Fig. 2 – Block diagram of proposed RF-FOFPID-based control strategy.

3.1. DESIGN OF FOFPID CONTROLLER

The closed loop PID-tuned PWM controller is developed to control the converter output voltage when the load fluctuates. The output voltage error values in the ITDC converter are regulated by optimizing the gain values of the FOFPID controller.

3.1.1. Fractional-order fuzzy pid controller

For the input SF, two gains, KD and KI, are introduced and serve as indicators of the output. Comparing this approach to other retired FLC-PIDs has several advantages. Figure 3 shows the block diagram of a fractional level fuzzy PID controller. The suggested method replaces a fractional order (μ) for the integral order (λ) at the output from the eFLC. This is the FO (sum) integration of the FLC outputs rather than the integer order error rate at the FLC input.

The above scheme's control law is provided as,

$$u_{FOPID-FLC}(t) = K_{PI}\frac{d^{-\lambda}u_{FLC}(t)}{dt^{-\lambda}} + \frac{d^{-\mu}u_{FLC}(t)}{dt^{-\mu}}K_{PD}\,. \quad (5)$$

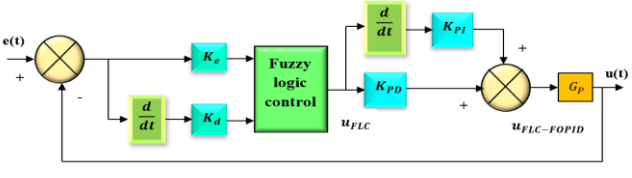

Fig. 3 – Block diagram of fractional order fuzzy PID controller.

3.2. PROPOSED RF-BASED FOFPID CONTROLLER CONTROL STRATEGY

The control signals are initially generated from the fuzzy controller according to the rule-based table corresponding to the input and desired output parameters. Meanwhile, the control signal generated from the FOPID controller while optimizing with the RF algorithm concerning the objective function developed. The consolidated control signals from fuzzy and RFA-tuned FOFPID controls are fed to the converter to regulate the output voltage. The flow chart of the proposed RF-tuned FOFPID controller strategy is shown in Fig. 4. The optimal tuning of the converter for effective voltage regulation is the proposed research problem. The lucrative ITSE objective function is proposed in [10]

$$\text{ITSE} = \int_0^t t \cdot e(t)^2 \mathrm{d}t. \tag{6}$$

The error signal, denoted $e(t)$, is the difference between the reference angular velocity and the actual angular velocity, where t is the simulation time.

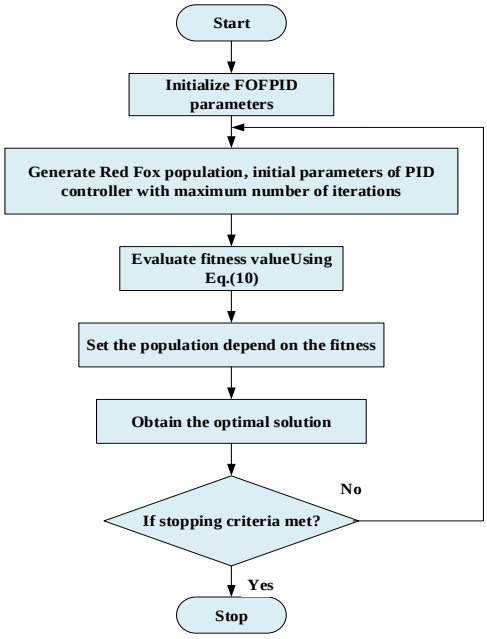

Fig. 4 – Block diagram representation of the proposed RF-FOFPID tuning approach.

3.1.2. Red fox algorithm (RFA)

The most efficient metaheuristic algorithm created recently is called RFA and is inspired by the nomadic hunting habits of red foxes [18–20]. The random initialization of particles in the solution space is the first step of this algorithm (11).

$$(X)^i = [(x_0)^i, (x_1)^i, \ldots \left((x_{n-1})^i\right]. \tag{7}$$

where i and t represent the size of the population and iterations. The global optimal solutions could be achieved when $f((X))^i$related to the minimization objective function (10) reaches the global minimum point. In the next stage, the red fox starts searching for food. The distance of each individual related to the best fitness values is found as follows (8), where $\bar{x}^i$ is the individual solution at i^{th} population and $\bar{x}^{best}$ is the best individual with the least fitness value, which is found after sorting the fitness value of everyone.

$$d\left((\bar{x}^i)^t, (\bar{x}^{best})^t\right) = \sqrt{\|((\bar{x}^i)^t - (\bar{x}^{best})^t)\|}. \tag{8}$$

The movement of individuals toward the best solution is represented as follows (9), where A is the randomly selected scaling parameter. The further movement of each individual is decided upon their fitness values after moving towards the best solution. If the fitness value of the new position is lower than the fitness value of the previously maintained individual, the individual will stay in that position; otherwise, they will return to their previous position.

$$\bar{x}^i)^t = (\bar{x}^i)^t + A \cdot Sn((\bar{x}^{best})^t - (\bar{x}^i)^t). \tag{9}$$

In local search, the red fox moves through its territory to search for possible prey locations. This movement is decided by a random scaling factor $\mu \in \langle 0, 1\rangle$ (10), where the radius of the hunting area is represented in equation (11). Here $\in \langle 0, 0.2\rangle$ is the angle of observation $\emptyset_0 \in \langle 0, 2\pi\rangle$, and θ is a random value between (0-1). The movements of individuals are stated below (12). The angular values of each individual are randomized between $\langle 0, 2\pi\rangle$

$$x_0^{new} = ar \cdot \cos(\emptyset_1) + x_0^{actul} \tag{10}$$

$$x_1^{new} = ar \cdot \sin(\emptyset_1) + ar \cdot \cos(\emptyset_2) + x_1^{actul}$$

$$x_2^{new} = ar \cdot \sin(\emptyset_1) + ar \cdot \sin(\emptyset_2) + ar \cdot \cos(\emptyset_3) + x_2^{actul}$$

…

$$x_{n-2}^{new} = ar \cdot \sum_{k=1}^{n-2} \sin(\emptyset_1) + ar \cdot \cos(\emptyset_{n-1}) + x_{n-2}^{actul} \tag{11}$$

$$x_{n-1}^{new} = ar \cdot \sin(\emptyset_1) + ar \cdot \sin(\emptyset_2) + \cdots ar \cdot \sin(\emptyset_{n-1}) + x_{n-1}^{actul} \tag{12}$$

Elimination and reproduction are the next stages, where the best survivors reproduce, and the worst are removed from the herd. The habitat of the best couples for reproduction and their Euclidean distance is represented in eq. (13) and (14).

$$(\text{habitat}^{\text{center}}) = \frac{(\bar{x}^1)^t + (\bar{x}^2)^t}{2}, \tag{13}$$

$$\left(\text{habitat}^{\text{dia}}\right) = \sqrt{\|(\bar{x}^1)^t + (\bar{x}^2)^t\|}. \tag{14}$$

Generating a new nomadic individual or reproducing an alpha couple depends on the random parameter $k \in \{0,1\}$. Each time, we take a random parameter $k \in \{0, 1\rangle$, specifying the iteration replacement according to

k – random parameter

$$\begin{cases} \text{new individual generation} & \text{if } k \geq 0.45 \\ \text{reproduction from couple} & \text{if } k < 0.45 \end{cases}. \tag{15}$$

4. **RESULTS AND DISCUSSIONS**

The Simulink model of a closed-loop converter with a FOPID controller is developed using the MATLAB software tool, and the controller gain values are optimized with the proposed RFA-based fuzzy controller. An array of 5 LEDs is connected in series, each with a power capacity of 10 watts. High-power LEDs require a resistive load to meet the required parameters. It is maintained at an 850 mA current, and the voltage across each input voltage varies from 8 V, 12 V, and 16 V, which are evaluated here. The graphical time variation for V, I of the proposed system is shown in Fig. 7. A comparison is made between the proposed RF-FOFPID controller and the traditional PID controller, fuzzy PID controller, and FOPID controller. The input voltage is 12 V, the output voltage is 97.5 V, the reference voltage is 75 V, and the switching frequency is 100 kHz. The population size of the red fox is 30, and the iteration is 1000.

Additionally, the proposed converter increases the steady-state response of the system by generating an output voltage of 97.5 V (notice the signal values at the locations indicated by the borders). The reference voltage determines the load resistor voltage. The converter system uses 75 V as a reference voltage.

According to the above Fig. 5, the proposed RF-FOFPID controller-based converter regulates the output voltage by

driving it to produce the desired value of 97.7…97.8 V and steady-state errors. Semiconductor devices are subjected to low voltage stress, low input current ripple, and high voltage gain when using the proposed boost converter. The proposed converter's L2C2D2 network increases the voltage gain of the device while reducing the voltage across the power switch. In addition to having a high-frequency ambient potential difference between input and output, the converter also has two power switches.

A plot of the voltage and current responses of the PID, Fuzzy PID, FOPID controllers, and the proposed RF-FOFPID controller is shown in Figs. 6–8.

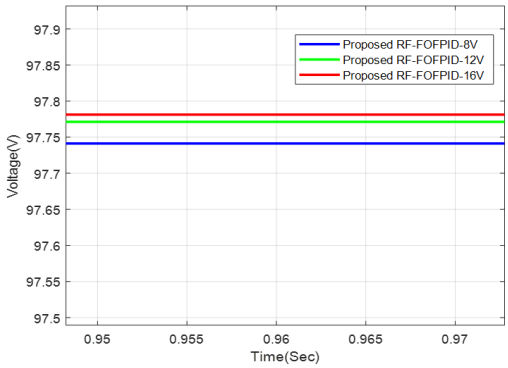

(a)

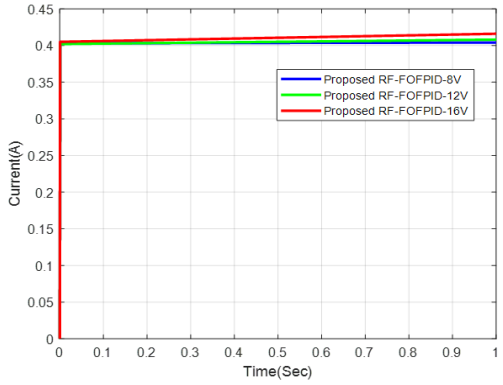

(b)

Fig. 5 – Regulated output response of: a) voltage; b) current using PID controller.

Voltage and current responses for both current and voltage applied to a 50 W LED string have been achieved.

Figure 6 illustrates the voltage and current response at LED current 850 mA. From the above results, the proposed RF-FOFPID controller-based converter performs better than the existing system.

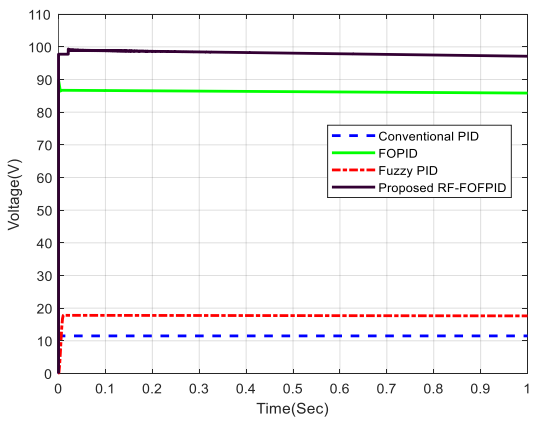

(a)

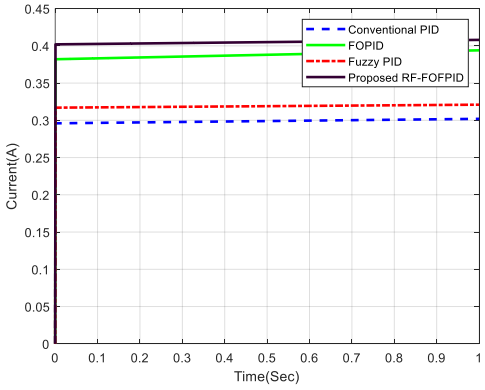

(b)

Fig. 6 – Output response of: a) voltage; b) current for LED current 850 mA.

The voltage and current response for an 8 V input voltage are shown in Fig. 7. The voltage and current response for a 16 V input voltage are shown in Fig. 8. From the above results, the proposed RF-FOFPID controller-based converter maintains the voltage in the range of 97.7…97.8 V, but the existing controllers slightly varied with vary desired output voltage.

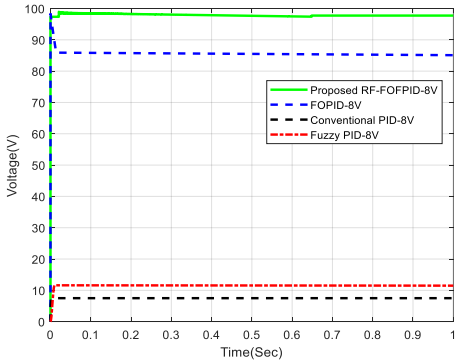

(a)

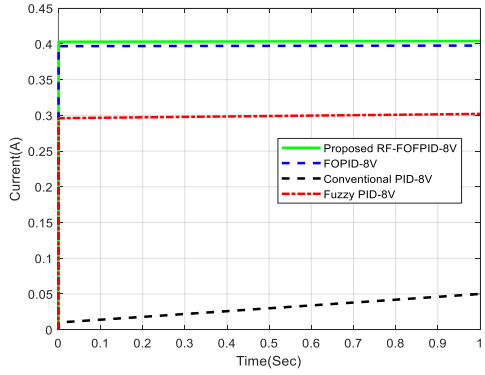

(b)

Fig. 7 – Output response of: a) voltage; b) current for input voltage at 8 V.

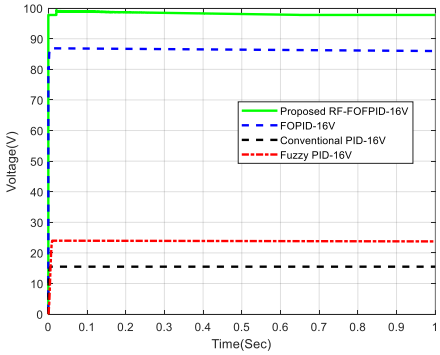

(a)

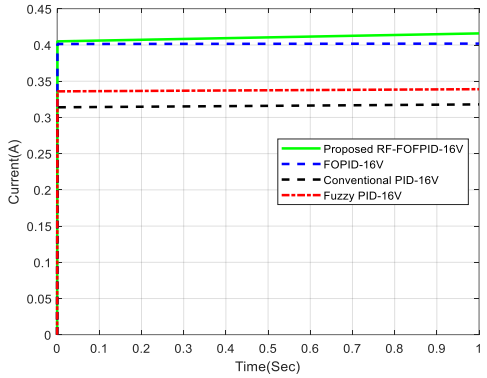

(b)

Fig. 8 – Output response of: a) voltage; b) current for input voltage at 16 V.

The output results indicate that peak overshoot, excessive settling time, and steady-state error always exist in conventional PID controllers. As K_p increases, the front end of the output voltage wave oscillates more intensely. A fuzzy PID controller and a fuzzy FOPID controller have been used to reduce the peak overshoot value, but it has not been completely removed. As a result, an improved transformer, a less DC-DC converter, was further tuned with the Red Fox algorithm to completely overcome peak overshoot, resulting in a faster, more efficient, and more dynamic response. In addition to eliminating the peak overshoot problem, the proposed controller provides another benefit. It has been reduced, but not completely, compared to the existing converter's peak overshoot. The system has only reached a certain level of stability. The converter's voltage gain is between 2 and 10, while its duty cycle is between 0.1 and 0.9. RF-FOFPID controller based on improved transformerless converter voltage gain. Due to the low variation rate of its coupling inductance, the proposed structure exhibits higher voltage gain than other structures.

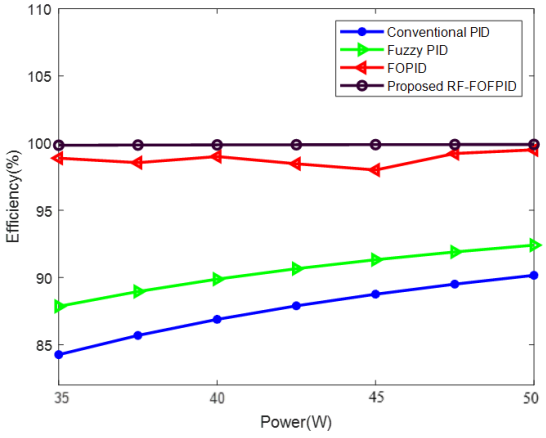

Fig. 9 – Efficiency comparison.

Based on the output power range of 35 W to 50 W, the performance of the specified converter and the compared converters are shown in Fig. 9. Compared to other structures with a full load condition, it is obvious that the recommended structure will achieve high efficiency. The fuzzy-PID controller-based transformerless converter achieves 92.57 %, the FOPID controller-based modified transformerless converter achieves 99 %, and the proposed RF-FOFPID-based ITDC converter efficiency is 99.9 % at 50 W (full load condition). The graph also shows that performance increases as the input voltage increases. Higher input voltage allows the converter to operate more efficiently. To save power, the current drops as the voltage rises.

By reducing the conduction losses across the diodes, switches, and resistances of the inductor and capacitor, the converter can reduce its power consumption. Besides, there are soft-switching conditions through the diodes of the presented converter, which leads to a further increase in efficiency.

Table 1

Optimized gain values

Controllers	K_P	K_I	K_D	λ	μ
RF-FOFPID	2.9987	3.9562	2.8798	0.9312	0.9533
FOPID	3.8124	1.4214	3.4423	0.9723	0.9982
Fuzzy PID	3.1221	2.5421	1.8567	-	-
PID	15	2.5	8	-	-

Table 2

Performance comparison

Controller	Overshoot [mA]	Settling time [s]	Rise time [s]	Steady-state error [mA]	ITSE
Proposed RF-FOFPID Controller	0.0011	0.0023	0.002	0.0034	0.0175
FOPID Controller	0.0052	0.0019	0.0023	0.006	0.0244
Fuzzy PID Controller	3	0.0065	0.0044	0.66	1.6351
PID Controller	2	0.0133	0.0101	1.46	4.2369

The RF-FOFPID controller gain values tuned with various metaheuristic approaches are shown in Table 1. As a basis for comparison, Table 2 presents the corresponding time domain specifications for standard PID, Fuzzy PID, FOPID, and RF-FOFPID controllers to make a better comparison. RF-FOFPID controllers provide more stable output voltages and improved regulation. The proposed RF-FOFPID controller is more robust than existing controllers when using ITAE measurement rule because of lower settlement times. All the improvements mentioned above are achieved with even lower control efforts. The proposed RF-FOFPID control-based converter greatly reduces transient disturbances and switching losses. The RF-FOFPID controller rejects this disturbance much better than the FOPID, PID, and fuzzy PID controller-based converter.

5. CONCLUSION

This work presents an improved transformerless dc-dc boost converter based on a new Red Fox optimized fractional order PID (FOFPID) controller to control a string of LEDs. The proposed study aims to control the converter's output voltage under fixed loads and varying input voltage conditions to provide the required voltage (97.7…97.8 V) for LED applications. Three simulation analyses were performed to evaluate the effectiveness of the proposed RF-FOFPID controller. This analysis's results confirm that the proposed controllers reduce more than 80 % of maximum peak overshoot, nearly 50 % of rising time, and 99 % of steady-state error area compared to the FOPID, PID, and fuzzy PID controller-based converter. Finally, the robustness of the LED driver circuit is considered and examined under variable load conditions. The test result of the RF-FOFPID controller in effective voltage regulation under wide variations of input voltage conditions. Hence, the successful voltage regulation of the LED driver circuit is obtained with

the proposed RF-FOFPID controller, and superiority is also proved with the FOPID, PID, and fuzzy PID controller-based converter. This work could be performed soon with a buck-boost converter with the same optimization algorithm. Instead, the objective functions incorporated the output parameters with adequate weighting factors that could be considered soon to study performance.

Received on 29 November 2023

REFERENCES

1. M. Zhao, Q. Zhang, Z. Xia, *Narrow-band emitters in LED backlights for liquid-crystal displays*, Materials Today, **40**, pp. 246–265 (2020).
2. Y. Huang, E.L. Hsiang, M. Y. Deng, S. T. Wu, *Mini-LED, micro-LED and OLED displays: present status and future perspectives*, Light: Science & Applications, **9**, *1*, pp. 1–16 (2020).
3. A. Tepljakov, B.B. Alagoz, C. Yeroglu, E. Gonzalez, S.H. Hossein Nia, E. Petlenkov, *FOPID controllers and their industrial applications: A survey of recent results*, IFAC-PapersOnLine, **51**, *4*, pp. 25–30 (2018).
4. Y. Arya, *A novel CFFOPI-FOPID controller for AGC performance enhancement of single and multi-area electric power systems*, ISA transactions, **100**, pp. 126–135 (2020).
5. A. Mohanty, M. Viswavandya, S. Mohanty, *An optimised FOPID controller for dynamic voltage stability and reactive power management in a stand-alone micro grid*, International Journal of Electrical Power & Energy Systems, **78**, pp. 524–536 (2016).
6. M.A. George, D.V. Kamat, C.P. Kurian, *Electronically tunable ACO based fuzzy FOPID controller for effective speed control of electric vehicle*, IEEE Access, **9**, pp. 73392–73412 (2021).
7. C. Zhou, Q. Zhang, D. Ezechias, Y. Gao, H. Deng, S. Qu, *A general digital PID controller based on PWM for buck converter*, in Proceeding of the 11th World Congress on Intelligent Control and Automation, IEEE, pp. 4596–4599 (2014).
8. W. Widonarko, G.A. Rahardi, C. Avian, W. Hadi, D. W. Herdianto, P.L. Satrio, *Driver for led lamp with buck converter controlled by PID*, International Seminar on Intelligent Technology and Its Applications (ISITIA).
9. C.C. Raicu, G.C. Seritan, B.A. Enache, *48 V network adoption for automotive lighting systems* Rev. Roum. Sci. Techn. – Électrotechn. et Énerg., **66**, *4*, pp. 231–236 (2021).
10. S.V. Adhul, T. Ananthan, *FOPID controller for buck converter*, Procedia Computer Science, **171**, pp.576-582 (2020).
11. A. Chakrabarti, P.K. Sadhu, P. Pal, *A novel dead-time elimination strategy for voltage source inverters in induction heating systems through fractional order controllers*, Rev. Roum. Sci. Techn. – Électrotechn. et Énerg., **67**, *2*, pp. 181–185 (2022).
12. C. Demircan, O.V. Güler, A. Keçebaş, *Meta-heuristic algorithm-based optimal PID controller design for power converters*, Advances in Artificial Intelligence Research, **1**, *2*, pp. 67–72 (2021).
13. M.E. Çimen, Z.B. Garip, A.F. Boz, *Chaotic flower pollination algorithm based optimal PID controller design for a buck converter*, Analog Integrated Circuits and Signal Processing, **107**, *2*, pp. 281–298 (2021).
14. S.M. Ghamari, H.G. Narm, H. Mollaee, *Fractional-order fuzzy PID controller design on buck converter with antlion optimization algorithm*, IET Control Theory & Applications, **16**, *3*, pp. 340–352 (2022).
15. P. Warrier, P. Shah, *Optimal fractional PID controller for buck converter using cohort intelligent algorithm*, Applied System Innovation, **4**, *3*, p. 50 (2021).
16. L.C. Borin, E. Mattos, C.R. Osorio, G.G. Koch, V.F. Montagner, *Robust PID controllers optimized by PSO algorithm for power converters*, in IEEE 15th Brazilian Power Electronics Conference and 5th IEEE Southern Power Electronics Conference (COBEP/SPEC), pp. 1–6 (2019).
17. A.M.S.S. Andrade, T.M.K. Faistel, R.A. Guisso, A. Toebe, *Hybrid high voltage gain transformerless dc–dc converter*, IEEE Transactions on Industrial Electronics, **69**, *3*, pp. 2470–2479 (2021).
18. L.S. Yang, T.J. Liang, J.F. Chen, *Transformerless dc–dc converters with high step-up voltage gain*, IEEE Transactions on Industrial Electronics, **56**, *8*, pp. 3144-3152 (2009).
19. D. Połap, M. Woźniak, *Red fox optimization algorithm*, Expert Systems with Applications, **166**, p. 114107 (2021).
20. J.G. Malar, V. Thiyagarajan, N.B.M. Selvan, M.D. Raj, *Electric vehicle onboard charging via Harris hawks optimization-based fractional-order sliding mode controller*, Rev. Roum. Sci. Techn. – Électrotechn. et Énerg., **68**, *1*, pp. 30–35 (2023).